Design and Implementation of a Chassis Dynamometer for Testing Battery-Powered Motorcycles

DING-TSAIR SU, YING-SHING SHIAO, JUI-LIANG YANG
Department of Electrical Engineering
National Changhua University of Education
No. 2 Shi-Da Rd., Changhua City, 500 Taiwan
REPUBLIC OF CHINA (TAIWAN)
sdt@ctu.edu.tw, http://www.ncue.edu.tw

Abstract: - The objective of this paper is to design and implement a chassis dynamometer for testing dynamic characteristics of a battery-powered motorcycle (BPM). By using a load simulation system, which is constituted with a DC motor and two rollers, a roller of the test platform is connected to a DC motor through a torque sensor, and a controller is designed to control the DC motor to simulate driving resistance produced when the BPM runs on various roads. The test platform can simulate each drag force when the BPM is in acceleration or in a constant-speed drive, and also can simulate kinetic energy gained by the BPM when braking, deceleration and running downhill. A computer not only controls the test platform but also collects signals from sensors on the test platform and the BPM, and can analyze related data such as driving resistance, driving range, speed, kinetic energy recycle and so on. The test platform has an integral steel structure and a stable center of gravity, and the height and length adjustment of the machine is convenient and as well the test is easy to perform, thus it can provide efficient tests on battery-powered motorcycles (BPMs) which are currently popularized by all circles with great efforts, so as to achieve the objective of performance measurement, performance analysis and data collection. From experiment results, the BPM performance test platform can simulate various road patterns and complete an automatic testing process.

Key-Words: - Chassis dynamometer, Battery-powered motorcycle, Test platform, Driving resistance, Drag force, Kinetic energy recycle, Road patterns.

1 Introduction

Because of the particular geographic environment and life habitual behavior, as well as the centralization of city population and the characteristic of the traffic system, the growing number of motorcycles is amazing in Taiwan. According to statistical data, the number of motorcycles in Taiwan is only next to that of Japan and is second in the world; however, the density of motorcycles on roads is number one in the world. The yearly amount of exhaust from these motorcycles becomes the main moving pollution source in the city, resulting in an air pollution issue, which seriously threatens human health and existence, but the battery-powered motorcycle (BPM) is one of the most direct and effective solutions to this issue [1, 2]. Because related technical development in the Taiwan motorcycle industry is quite mature, it is very suitable to popularize the BPM. Therefore, based on cooperation with the government policy and integration with research development of academic circles and civil industries, it is hopeful that Taiwan will have the fastest development in BPMs and becomes the most important productive country of BPMs in the world.

The basic performance requirements of BPMs are: maximum speed, driving range and acceleration. Performance requirements of batteries are: high energy density, high output power density, increased recycling usage life, reduced charging time, high energy efficiency, low self-discharge rate and maintenance-free. However, the energy density of batteries for BPMs is much lower than that of gasoline, resulting in lower performance of commercial running BPMs compared to that of general internal-combustion vehicles [3-5]. Therefore, increasing system efficiency by energy management can increase driving mileages of BPMs [6-8].

Presently, test platforms for electric vehicles are generally divided into chassis-type and engine-type platforms. In an engine-type test platform, a dynamometer is coupled directly to the engine of a vehicle under testing to simulate the load on the engine and gearshift in the gearbox. In a chassis-type test platform, however, the dynamometer makes contact with the tires of an electric vehicle

via rollers so as to simulate the actual load from the road. Now that some BPMs use continuously variable speed transmission systems, in which gear ratios are changed continuously according to the speed and load of the vehicles at any time rather than through fixed gear positions, it is difficult to design an engine-type test platform that must also consider and simulate the continuously variable speed transmission of such as electric motorcycles. In addition, a BPM must be disassembled before it can be tested on an engine-type test platform, which is very inconvenient [9-13]. Therefore, the test platform design in this paper is focused on the chassis-type test platforms.

The main objective of this paper is to research and design a test platform to directly test the performance of BPMs in labs, so that the inconvenience of road tests is reduced and then the research and development of BPMs are accelerated. The test platform as designed in this paper can simulate various road patterns like in the city, in the suburbs, running uphill and running downhill. Therefore, test conditions of BPMs in this test platform are requested to be as same as possible to real road test conditions, and besides, for BPMs, important test items like the acceleration characteristics and the driving resistance and kinetic energy produced when decelerating or braking can be tested accurately.

2 Configuration of the Test System

When a BPM runs, the overall efficiency affects the driving mileage. Therefore, the discharge efficiency of batteries, the operation efficiency and road patterns are very relative to one another [7]. In this paper, a performance test platform is designed to test driving characteristics of a BPM, and the operation mode of the DC motor on the platform is controlled to simulate driving resistance of BPMs running on various road patterns.

A configuration of the performance test system is as shown in Fig. 1. When the BPM is accelerating, running uphill or running at constant speed, the DC motor on the platform is driven by the BPM wheel through the coupler and operates in a DC generator mode. The output power of the generator passes through the regenerative controlled circuit composed by S_1, S_2, S_3 and S_4 and is transformed from DC to AC power, and is transmitted back to the utility (AC 220V). Controlling the magnitude of regenerative electricity can produce various drag torques. Thus, the DC motor of the test platform provides a driving resistance opposite to the driving direction regarding the BPM. The electricity feedback to the utility side from the regenerative controlled circuit means the electricity consumption of the driving resistance.

When the BPM is decelerating, braking or running downhill, a semi-converter composed of S_5, S_6, D_1, D_2 and D_3 is driven by a phase controlled and transforms the AC to DC for the DC motor. The DC motor operates in the motor mode and drives the BPM wheel to continue moving forward, but the speed is smoothly decreasing to zero. Therefore, the DC motor on the test platform provides a driving force in the moving direction of the BPM to simulate the kinetic energy produced when the BPM is cruising, braking or running downhill, and the consume energy index of various driving modes of the BPM can be measured simultaneously. The measurement of the state of charge is an important basis of monitoring energy consumption. The purpose of energy management is to calculate the driving mode with the highest efficiency. Certainly, considering driving safety, the driver controls the speed and the optimum speed calculated by the energy management system is only a reference to the driver.

3 Control System Analysis

When the BPM is running, the electricity is transformed to kinetic energy to overcome the driving resistance. Driving resistance includes rolling friction resistance, air resistance, moment of inertia, and uphill resistance and so on. Fig. 2 is showing the driving resistance of BPM, wherein the rolling friction resistance F_r is expressed in (1):

$$F_r = \mu Mg \cos\theta \tag{1}$$

In (1), μ is the coefficient of rolling friction resistance, M is the total mass of the vehicle and rider, g is the acceleration of gravity, and θ is the included angle of the road surface and the horizontal line.

When the motorcycle is running forward, the resistance produced from the vehicle external surface and the air is the air resistance F_a, as expressed in (2):

$$F_a = \rho C_d S \frac{v^2}{2} \tag{2}$$

In (2), ρ is the air density, v is the vehicle speed, C_d is the coefficient of air resistance, and S is the orthogonal projection area of the rider to the vehicle moving direction. Because the BPM shape is irregular, the shape of the rider, riding posture and

the clothes worn by the rider all affect the orthogonal projection area and the coefficient of air resistance. Thus, to simplify variables, the CNS test standard specifies the air resistance $F_a = C \times v^2$, in which the C value is affected by the vehicle weight [2].

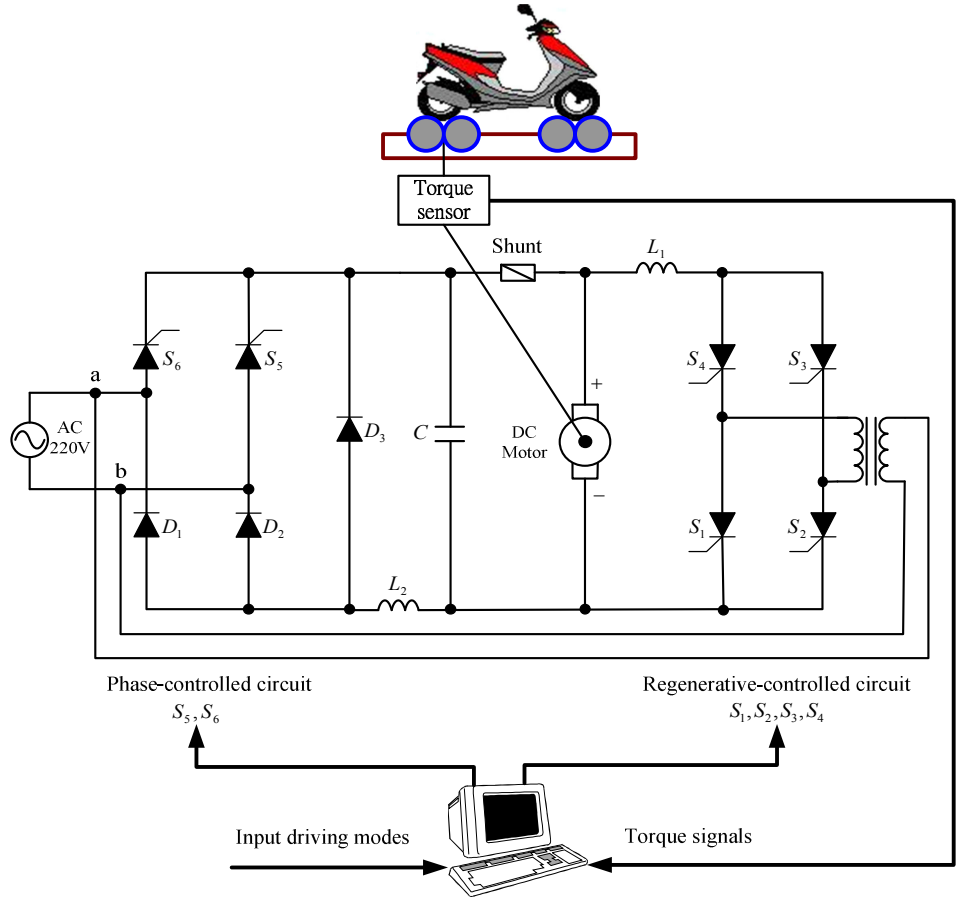

Fig. 1 The setup of the BPM performance test system

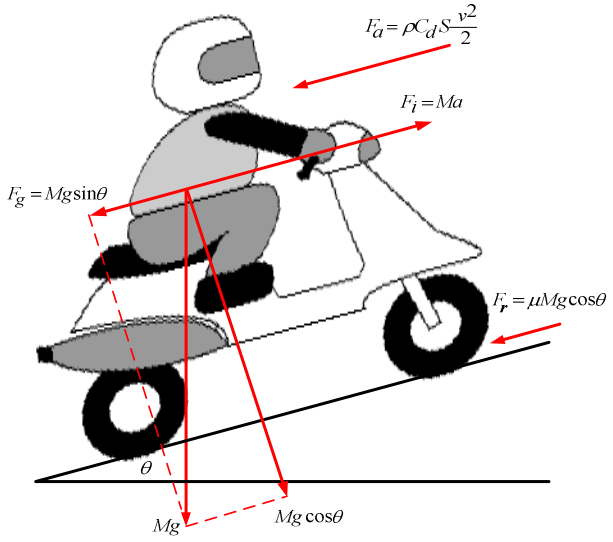

Fig. 2 The diagram of driving resistance for BPM

The uphill resistance is expressed in (3):

$$F_g = Mg\sin\theta \tag{3}$$

As the driving force of the motor overcomes the rolling friction resistance, air resistance and uphill resistance, the remaining driving force represents the moment of inertia, which is expressed in (4), wherein a is the driving acceleration.

$$F_i = Ma \tag{4}$$

To summarize each driving resistance mentioned above, the uphill resistance F_g is related to the road surface inclination angle θ. The air resistance F_a is in direct proportion to the square of vehicle speed, being very small when the speed is low, but is the most driving resistance when the speed is high. The rolling friction resistance F_r is like the maximum static friction force, the vehicle starts to move after the driving force overcomes the rolling friction resistance F_r. After the vehicle starts

to move, most driving force is spent on the acceleration until the constant acceleration a equals zero, then the acceleration resistance is also zero, at the moment the driving force equals the sum of the other three resistance forces. The driving resistance of the overall vehicle is expressed by (5):

$$F_R = F_r + F_a + F_i + F_g \tag{5}$$

According to the driving resistance as design in (5), the drag-controlled system is as shown in Fig. 3. The rotational speed is calculated from encoder singles of the brushless DC motor on the BPM, and then is transformed to the vehicle speed signal v through $2\pi/60$, the wheel radius r and the teeth numbers ratio K_G, and then the inertia resistance F_i and the air resistance F_a are calculated after differentiation and square, and finally the driving resistance F_R of various road patterns is obtained by adding the friction resistance F_r and the uphill resistance F_g. According to the mechanical constant of the test platform, the driving resistance is transformed to a drag torque T_D needed to produce the driving resistance, and then is compared with the torque sensor feedback signal T_O on the transmission shaft of the test platform to produce a torque difference signal, so as to control a conducting angel of the S_1, S_2, S_3 and S_4 of the regenerative-controlled circuit (RCC) in Fig. 1 for the generator to output the current to produce the drag torque needed, thereby the roller of the test platform produced the correct driving resistance.

When the BPM is decelerating, braking or running downhill, the moment of inertia or gravity makes the BPM cruise forward, making the roller on the test platform to produce a driving force to the wheel of the BPM for simulation. The driving force is produced from the semi-converter. The semi-converter is composed of S_5, S_6, D_1, D_2, D_3 and a phase-controlled circuit (PCC) to provide DC power to the DC motor, for the DC motor to operate in the motor mode and drive the wheel of the BPM to produce the driving resistance when cruising, braking or running downhill. The test platform simulates the driving resistance when the BPM decelerating, braking or running down hill. The drive controlled system structure is as shown in Fig. 4, and the control method thereof is the same as that in Fig. 3 in substance, while the difference is that the moment of inertia and the uphill resistance are negative when cruising, braking or running downhill.

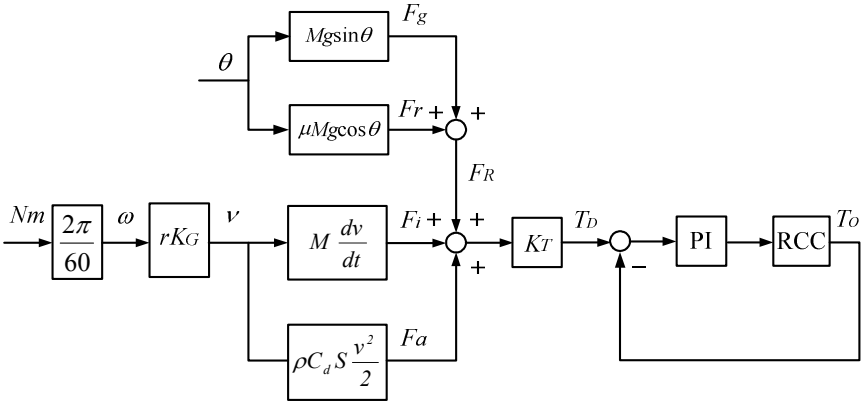

Fig. 3 The drag-controlled system

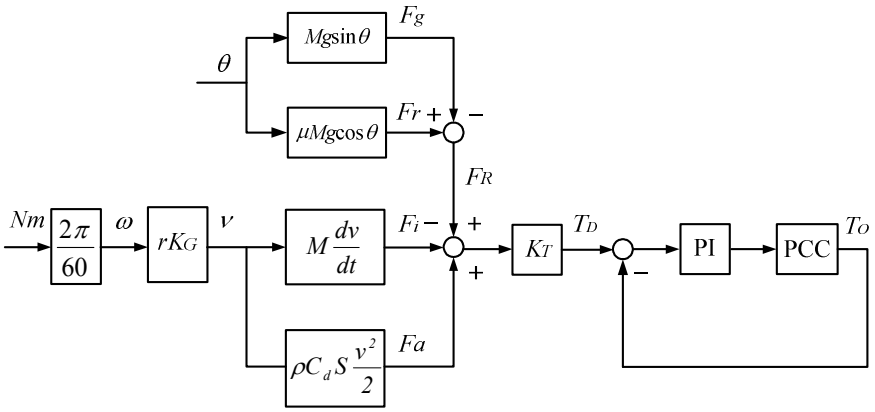

Fig. 4 The drive-controlled system

4 Design of the Control Program

In this paper, LabVIEW is used to design the operating program of the BPM test platform, and the controlling process is as shown in Fig. 5. First, the encoder A-phase signals of the brushless DC motor of the BPM is obtained, then the number of pulses within one second of the A-phase is calculated to obtain the speed N_m (rpm). Then, N_m multiplied by $2\pi/60$, the wheel radius r (20cm) and the teeth numbers ratio K_G (0.6) is the vehicle speed v. After the v is obtained, each driving resistance can be calculated.

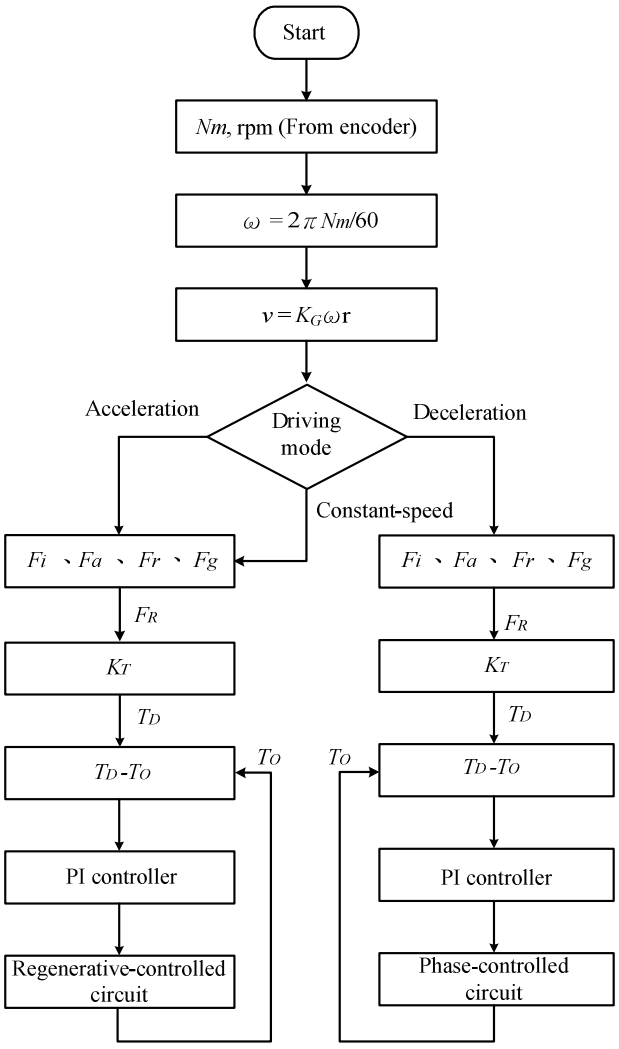

Fig. 5 The program controlling flowchart of the test platform

After the driving resistances are obtained when the BPM stops, accelerates, runs at a constant speed and decelerates, the driving resistance is transformed to the required drag torque T_D according to the mechanical constant (K_T = 0.2) of the test platform. The output signal T_O of the torque sensor on the transmission shaft of the test platform is measured and then compared to the output drag torque, and a control signal is outputted through the PI controller as in Fig. 5 to be transmitted to the regenerative-controlled circuit or phase-controlled circuit to produce correct T_O. The T_D-T_O torque error signal is inputted to a PI controller, and coefficients of the numerator and the denominator of the PI controller are respectively set in the program. The output signal of the PI controller is transmitted to the phase-controlled circuit or regenerative-controlled circuit through D/A card. When the BPM is accelerating or running at a constant speed, the output signals control the regenerative controlled circuit of the test platform. When the BPM is decelerating, the output signals control the phase- controlled circuit of the test platform.

5 Measurement of the Test Platform Parameters

When the BPM is tested on the test platform, the test platform needs to produce a correct driving resistance, and therefore the test platform parameters have to be obtained before testing the BPMs. As shown in Fig. 1, when the BPM is accelerating or decelerating, the regenerative-controlled circuit or the phase-controlled circuit on the test platform is controlled respectively to produce the correct driving resistance as expressed by (5). The relationship of the torque sensor and the driving resistance in Fig. 1 is shown in detail in Fig. 6, and each side of the torque sensor is connected to the roller and the DC motor of the test platform respectively. When the BPM is accelerating, the torque T produced from the roller side is greater than the drag torque T_e produced by the DC motor, and the resistance torque measured by the torque sensor multiplied by the torque constant K_T is the driving resistance F_R of the BPM. On the contrary, when the BPM is decelerating, the drag torque T_e produced from the DC motor controlled by the phase-controlled circuit is greater than the braking torque produced from the motorcycle until the BPM stops.

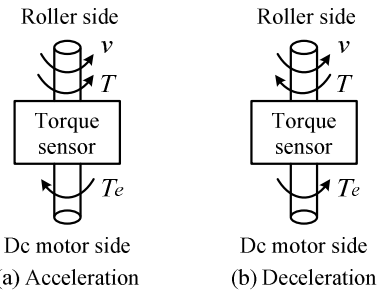

Fig. 6 The diagram of driving resistance

When accelerating, the BPM drives the DC motor connected on the platform to operate in a generator mode as shown in Fig. 7. $T\omega$ is the input of the DC motor (driven by the BPM), and the output power of the DC motor is $V_{DC} \times I_a$. The relationship of the driving torque T of the BPM, the drag torque T_e produced by the DC motor, the moment of inertia J_G and the viscosity frication coefficient B_m is expressed by the (6) and (7).

$$T = T_e + J_G \frac{d\omega}{dt} + B_m \omega \tag{6}$$

$$T\omega = V_{DC} I_a + I_a{}^2 R_a \tag{7}$$

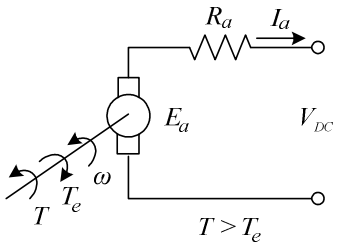

Fig. 7 DC motor operating in the generator mode

When the BPM is decelerating, the DC motor on the platform operates in the motor mode, as shown in Fig. 8, VI is the input power of the DC motor and $T_e\omega$ is the output power of the DC motor. The relationship of the torque T_e outputted from the DC motor on the platform, the drag torque T produced from the wheel, the J_M and the B_m is expressed by (8) and (9).

$$T_e = T + J_M \frac{d\omega}{dt} + B_m \omega \tag{8}$$

$$T_e\omega = VI - I^2 R_a \tag{9}$$

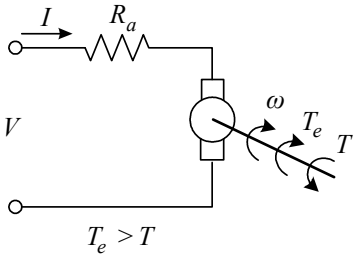

Fig. 8 DC motor operating in the motor mode

When the BPM is controlled by (6) to run at a constant speed, the B_m can be measured. The voltage and current of the battery on the BPM are measured by the D/A card, and one multiplied by the other is the rotating power P of the BPM. Ignoring the motor efficiency of the BPM, P divided by the angular speed ω_{BPM} equals the BPM driving torque T. Subtract T by the drag torque T_e generated by the DC motor, and then divided by the test platform speed ω_{TP} equals B_m. The calculation method is as shown in Fig. 9.

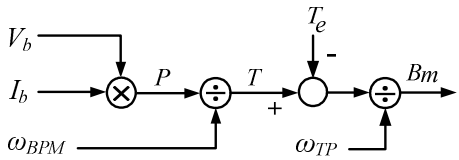

Fig. 9 Calculation method of the viscosity frication coefficient B_m

6 Experiment Results

As shown in Fig. 10(a) and 10(b), the B_m is 3~5kg · m^2/s, 1.8kg · m^2/s , 1kg · m^2/s and 0.8kg · m^2/s when the vehicle speed is 50rpm, 100rpm, 150rpm and 200rpm respectively. Because the B_m at speed 50rpm is inaccurate, in this paper, the other three data are taken to obtain an average of B_m which is 1.2 kg · m^2/s.

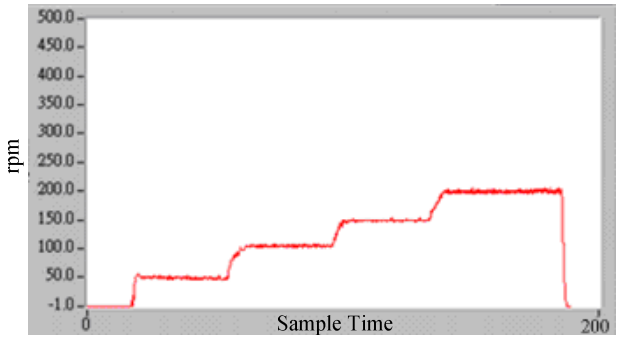

(a) Speed of the BPM

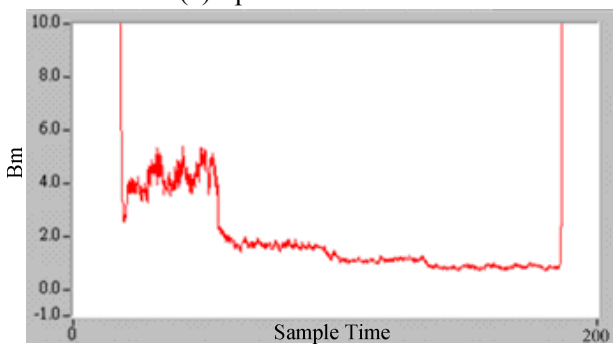

(b) Viscosity frication coefficient

Fig. 10 Test results of viscosity frication coefficient

The other experiment is to obtain the internal resistance R_a of the DC motor. The DC motor connected to the platform works as a generator, and the shunt-excited flux field of the DC motor is supplied with DC 200V, while the armature thereof

is connected a lamp load, and the BPM runs at a constant speed 200rpm. Then, the voltage and current at the armature terminals of DC motor for the test platform, as well as the output torque signal of the torque sensor, are measured respectively as shown in Fig. 11. The velocity of the BPM is ω_{BPM} = 20.93(rad/sec), and the armature voltage E_a is 48.2V, while the current I_a is 2A. The specification of the torque sensor is 10V/50N-m, and the voltage measured is 0.95V, so that T_e equals 4.75N-m after transformation. R_a is 0.754Ω after the above data substitute for the parameters in (7).

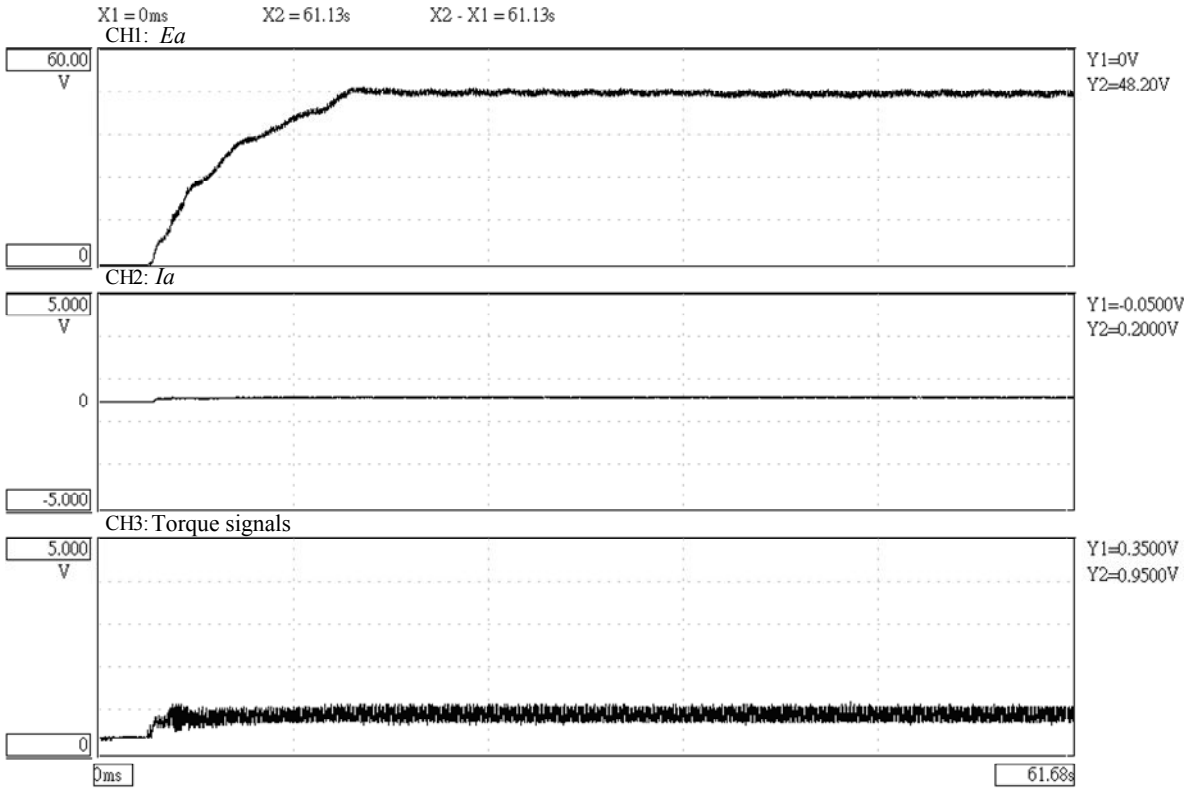

Fig. 11 The E_a and I_a of DC motor and the output signals of torque sensor

After measurement and calculation of the viscosity frication coefficient B_m and the internal resistance R_a of the DC motor, during the acceleration or deceleration process of the BPM, the moment of inertia J_G and J_M are measured and B_m and R_a substitute the corresponding parameters in (6) to (9) respectively. The calculation method is as shown in Fig. 12 and Fig. 13.

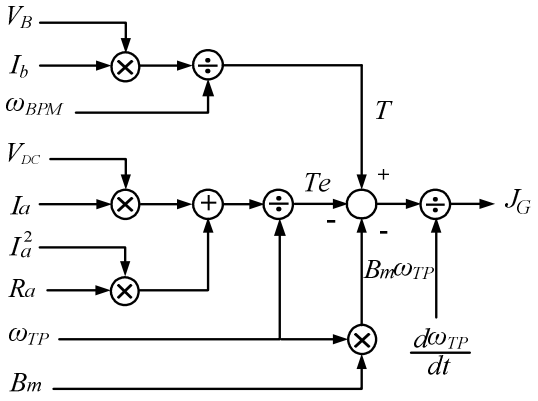

Fig. 12 Calculation method of moment of inertia J_G

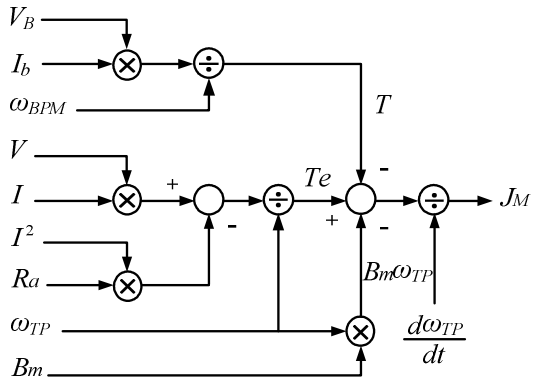

Fig. 13 Calculation method of moment of inertia J_M

The BPM runs in the driving modes (a) and (b) in Fig. 14 respectively, as shown in Fig. 15(a) and 15(c). The moment of inertia J_G and J_M are calculated as shown in Fig. 15(b) and 15(d). When the BPM is accelerated from zero to 5km/hr or 10km/hr, the moment of inertia measured is about 0.89kg · m^2 and 1.15kg · m^2 respectively, and the average is 1.02kg · m^2 as the moment of inertia J_G of the test

platform. When the BPM decelerates from 5km/hr or 10km/hr to 0km/hr, the moment of inertia J_M measured is about 0.76kg • m^2 and 0.93kg • m^2 respectively, and the average is 0.845kg • m^2 as the moment of inertia J_M.

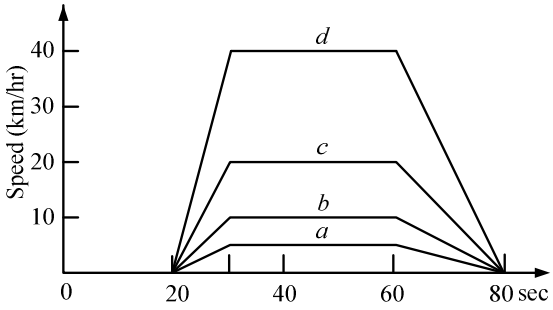

Fig. 14 Driving modes

The test platform can be controlled to produce the correct driving resistance after the parameters of the BPM test platform are obtained. When the BPM runs in the driving mode *a* and *b* respectively, the driving resistances obtained are as shown in Fig. 16(b), 16(c) and Fig. 17(b), 17(c). When the BPM stops, the driving resistance is 0 (N-m), and the speed of BPM accelerates to 5km/hr, the driving resistance increases from about 3.5N-m to 5.5N-m as shown in Fig. 16(b). When the speed of the BPM is at 10km/hr, the driving resistance increases from 3.5N-m to 12N-m because the speed increases. When the speed is at 5km/hr and 10km/hr, the driving resistances are about 5N-m and 10N-m respectively, as shown in Fig. 16(b) and Fig. 17(b). As the BPM decelerates to stop, the driving resistances are about from -0.5N-m to -2.5N-m and from 5N-m to -2.5N-m respectively, as shown in Fig. 16(c) and Fig. 17(c). It can be realized that from the above experiments, the test platform of the BPM can produce the correct driving resistance.

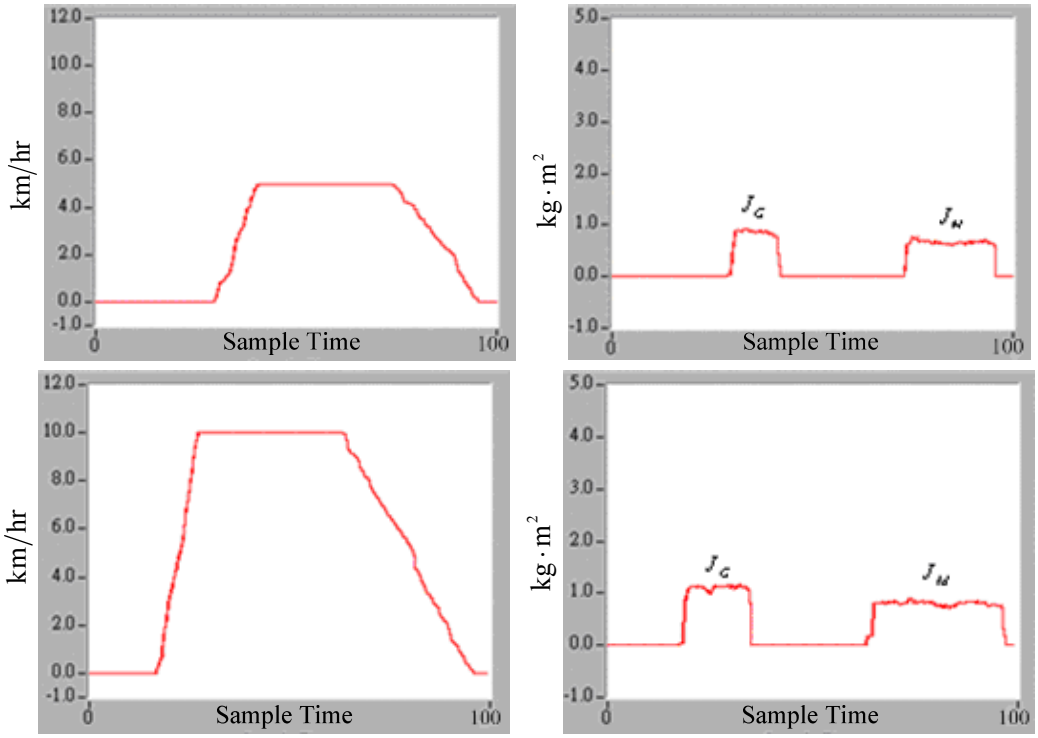

(a) Driving mode *a* (b) Moment of inertia J_G and J_M
(c) Driving mode *b* (d) Moment of inertia J_G and J_M

Fig. 15 Test results of the BPM in driving modes

7 Conclusions

The BPM performance test platform in this paper is designed with an adjustable steel structure, integrating the virtual control program design software LabVIEW, and operates in coordination with the D/A card to achieve the measurement and control of the system. The BPM is set up on the test platform, and then the test platform is controlled to produce the correct driving resistance, so as to simulate various road patterns, that is, to simulate various possible driving resistances when the BPM is running, so that the measurement of the consume energy index of the BPM can be performed in the

lab, as well as the parameters of the test platform can be measured correctly to be the reference for energy management and performance test. Meanwhile, efficient tests can be performed on BPMs currently popularized by all circles with great efforts, so as to achieve the objectives of fast and correct performance measurement and analysis as well as the data collection.

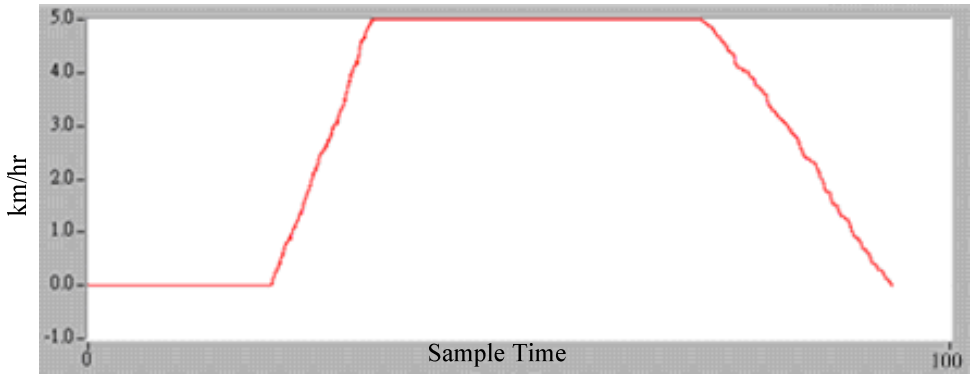

(a) Driving mode at 5km/hr

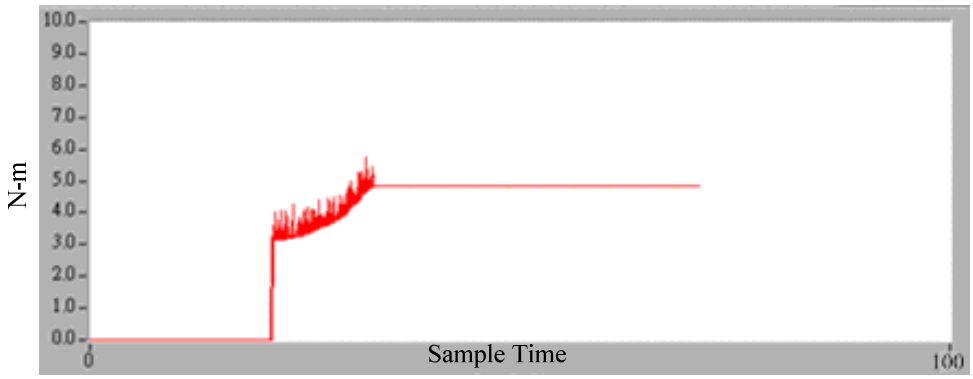

(b) Driving resistances when accelerating and running at constant speed

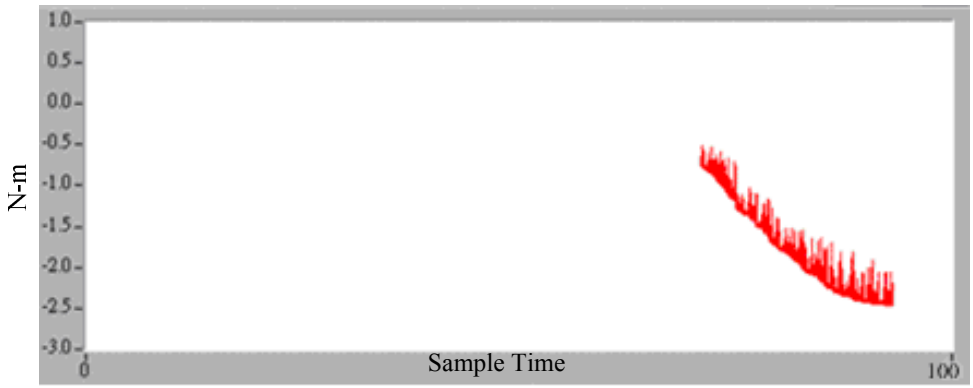

(c) Driving resistance when decelerating

Fig. 16 Controlling the test platform to produce driving resistances (Mode a)

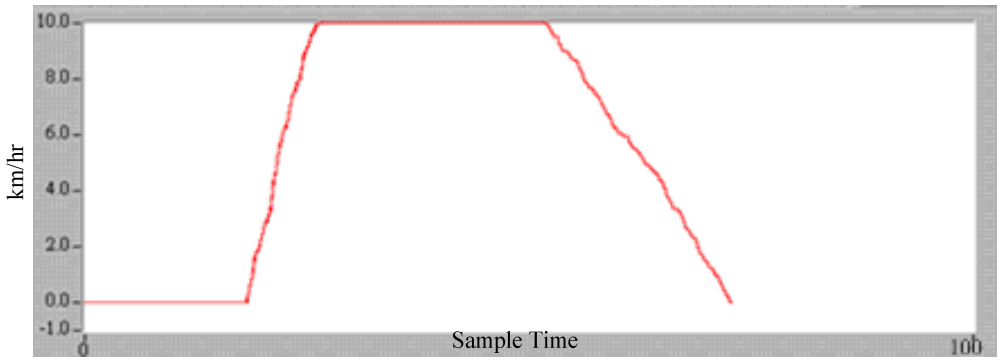

(a) Driving mode at 10km/hr

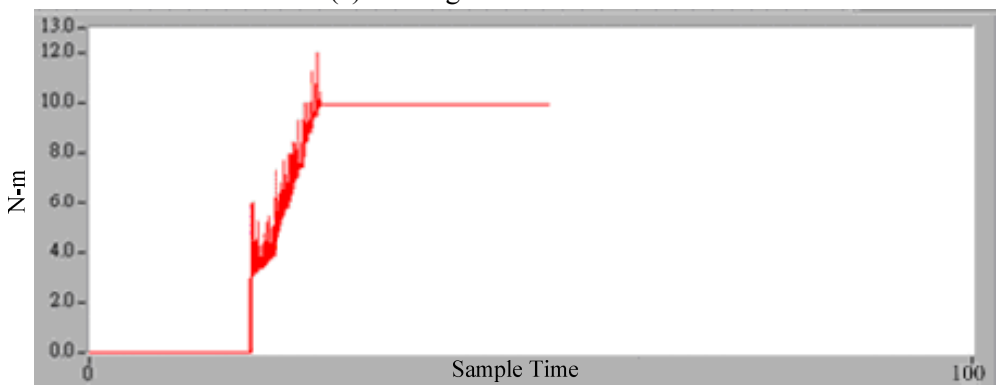

(b) Driving resistances when accelerating and running at constant speed

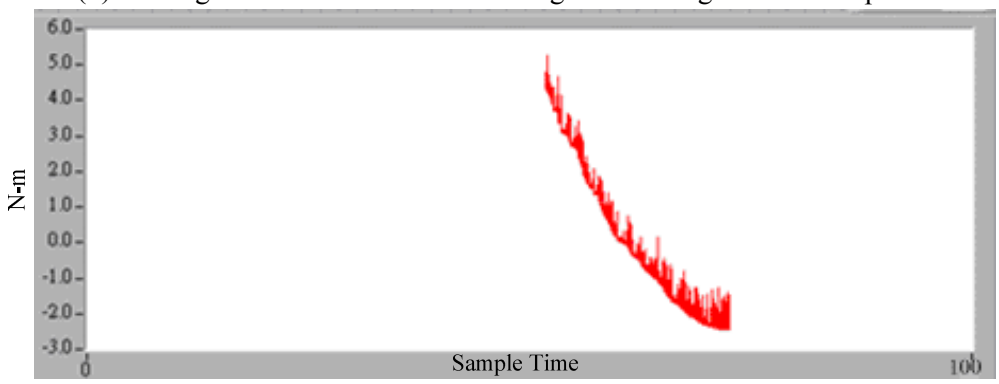

(c) Driving resistance when decelerating

Fig. 17 Controlling the test platform to produce driving resistances (Mode b)

References:

[1] C. C. Chan, An Overview of Electric Vehicle Technology, *IEEE Proceeding*, Vol. 9, 1995, pp. 1202-1207.

[2] Malledant, Specific Architectures for Electric Vehicles, *Proceeding EVS-13, Osaka*, Vo1. 2, 1996, pp. 119-125.

[3] C. C. Chan, Novel Wide Range Speed Control of Magnet Brushless Motor Drives, *IEEE Trans. On Power Electronics*, Vol. 10, No. 5, 1999, pp. 539-546.

[4] Y. S. Shiao, C. H. Huang, and C. W. Wang, The Propulsion Analysis and Regenerative Braking Controller Design and Implement for Battery Electric Motorcycles, *20th Symposium on Electrical Power Engineering*, Taipei, Taiwan, ROC, 1999, pp. 1-5.

[5] B. G. Cao, Z. F. Bai, and W. Zhang, Research on Control for Regenerative Braking of Electric Vehicle, *IEEE International Conference on Vehicular Electronics and Safety*, October 2005, pp. 92-97.

[6] N. Jinrui, S. Fengchun, and R. Qinglian, A Study of Energy Management System of Electric Vehicles, *IEEE Vehicle Power and Propulsion Conference*, September 2006, pp. 1-6.

[7] J. A. Ghaeb and O. M. Aloquili, New PWM Switching Technique for an Optimum Inverter Operation, *WSEAS Trans. on Systems and Control*, Vol. 3, Issue 5, May 2008, pp.

403-412.

[8] J. S. Won and R. Langari, Intelligent Energy Management Agent for a Parallel Hybrid Vehicle-Part II: Torque Distribution, Charge Sustenance Strategies, and Performance Results, *IEEE Trans. on Vehicular Technology*, Vol. 54, No. 3, May 2005, pp. 935-953.

[9] M. Ceraolo and G. Pede, Techniques for Estimating the Residual Range of an Electric Vehicle, *IEEE Trans. on Vehicular Technology*, Vol. 50, No. 1, January 2001, pp. 109-115.

[10] Y. P. Yang and T. H. Hu, A New Energy Management System of Directly-Driven Electric Vehicle with Electronic Gearshift and Regenerative Braking, *American Control Conference, ACC '07*, July 2007, pp. 4419-4424.

[11] G. Livint, V. Horga, M. Albu, and M. Ratoi, Testing Possibilities of Control Algorithms for Hybrid Electric Vehicles, *Proceedings of the 2nd WSEAS International Conference on Dynamical Systems and Control*, October, 2006, pp. 47-52.

[12] K. J. Kelly, M. Mihalic, and M. Zolot, Battery Usage and Thermal Performance of the Toyota Prius and Honda Insight During Chassis Dynamometer Testing, *The Seventeenth Annual Battery Conference on Applications and Advances*, January 2002, pp. 247-252.

[13] H. Rigakis, M. Vogiatzaki, J. Chatzakis, N. Lyberakisi, and M. Manitis, Test Pattern Designing Software for Electrical Appliance Testing Platform, *Proceedings of the 7th WSEAS International Conference on Applied Informatics and Communications*, August 2007, pp. 236-241.